Effect of inorganic particles on paint latex to form a VOC-free exterior water-based coating

Nathaniel Chin Yi Xuan[1], Ritwik Panigrahi[2], Thoniyot Praveen[2],

[1]H3 NUS-A*STAR-NJC Science Research Student, National Junior College

[2]Institute of Chemical and Engineering Sciences, Polymer Engineering and Characterization
A*STAR - Agency for Science, Technology and Research

Abstract

While paint industries are moving toward water-based paints, to lower volatile organic compound (VOC) emissions, there still remains the large issue: they are unable to rid of VOCs entirely. This project presents a novel solution to tackle this problem, using polymer nanocomposites that form SiO_2-latex interactions, which have been shown to increase the glass transition temperature (T_g) of the composite system. With this change in T_g and interaction, VOC-containing coalescing agents are no longer needed and a zero-VOC emulsion water-borne paint is able to be produced. The viscoelastic properties of the Latex/SiO_2 nanocomposites were studied using dynamic mechanical analysis (DMA) tests. The complex modulus ($\varepsilon^*=\varepsilon'+i\varepsilon''$) was measured by the resultant strain of applied certain sinusoidal force to the materials. It was observed that the T_g shifted to higher values with increasing SiO_2 content as a result of limited segmental mobility, before a gradual decrease, where there was a higher jump in T_g for the SiO_2 (ø=10nm) nanocomposites than that of the SiO_2 (ø=200nm). A minimum film formation temperature (MFFT) bar was also used to measure the MFFT of the films, which were found to be below room temperature, ensuring that the films were able to coalesce easily. This thus provides a new alternative for paint formulation, where VOCs are no longer required.

1. Introduction

Due to heightened awareness of the harmful effects of volatile organic compounds (VOCs), there has been increasing efforts in reducing the usage of VOCs in industries, to protect both the global environment and human health. VOCs are carbon-based compounds that have high vapour pressure at room temperature. According to the European Union 2004/42/EC for Decorative and Vehicle Refinishing Paints (Decopaint Directive), a VOC is as an organic compound with a boiling point of less than 250 °C (Directive EU, 2004). They harm the environment by acting as ozone precursors reacting with nitrogen oxide and carbon monoxide to form tropospheric ozone that contributes to the greenhouse effect. They can also cause health effects in the short term such as eye and throat irritation; to even lung cancer and damage to the nervous system in the long run (US EPA, 2017; Buday, M., Cater, F., Foulkes, S., Prakash, N. S. O., & Wilson, D., 2010).

In the paint-manufacturing and coating industry, VOCs are used as organic solvents, contributing to 30-40% of the paint's weight, which have been shown to continually emit vapours into the air even after the paint had dried (de Hek, H., Zabel, K. H., & Geurink, P. J. A., 1998). In 2011, it was found that New England had over 109,980 tonnes of VOCs that were emitted from the coating industry alone (US EPA, 2017); in fact according to the EPA, the off-gassing from architectural coatings is estimated to account for about 9% of the VOC emissions from all consumer and commercial products (Ian J. Rogan, 2002). Many paints also carry many false "Zero-VOC" labels, because by regulation, they still can contain up to 5g/L of VOCs (Buday et al., 2010).

Paints are liquid compositions that when applied to a surface (substrate), will harden into a solid film. There are a few types of paints, mainly: powder coatings, solvent-based paints and water-based paints. Powder coatings are very different from conventional paints in that they do not require any solvents to hold the binders and fillers together. Instead, heat is used to create a hard and durable finish, while also emitting negligible amounts of VOCs, making it an environmentally friendly alternative (PCI 2016). However, since an oven is required for coating, it makes it almost impossible to coat large objects like walls and buildings, in addition to requiring high amounts of energy for heating. The high costs of equipment, such as a high voltage spray gun and an oven for the application process also steers many consumers away from using it as a common option for coating. Solvent-based paints, often referred to as "oil-based paints" or "alkyd (synthetic) paint", make use of organic

solvents in their composition. They provide a smooth and thick coating that is very resistant and durable to scuffs. However, such paints are largely problematic due to their long periods of drying and the harmful VOCs that are given off in the process, giving them a very strong odour. (Ian J. Rogan, 2002; Shawn Cole, 2011) Since they undergo autoxidation when drying, the paints are highly susceptible to brittleness and yellowing when they age (Irich Poth, 2002). Nowadays, most of these oil-paints have been replaced with water-based paints (Zhu, A., Cai, A., Yu, Z., & Zhou, W., 2008), which make use of polymer emulsions. Here, VOC solvents are replaced with water, while synthetic polymers dispersed within it (latex) via surfactants are used as its binders. They are cheaper alternatives to the oil-based paints with various benefits such as weaker odours, lower VOC content, non-flammable, quick-drying and are less likely to peel and crack (Shawn Cole, 2011). Yet, water-based paints are still flawed as they contain VOCs in the form of coalescing agents, which help binders form a film upon the evaporation of water.

Due to the superior properties and cost-effectiveness of water-based paints, this project focuses on the development of water-based emulsion paints, with the aim of getting rid of coalescing agents so as to develop an environmentally friendly, fully VOC-free exterior coating. A typical water-based paint will consist of the following components:

Dispersion Medium: In emulsion waterborne paints, they contain water which is used as a dispersion medium. This acts as a carrier for the binders and inorganic components, and will not become part of the film. Instead, it helps to adjust the viscosity of the paint, allowing the latter to be applied before evaporating off. The coalescing of pigments and binders are then able to begin the film formation process.

Binders: The binders are the film-forming components of the paint, which help to impart adhesion. In waterborne paints, polymers dispersed in water, known as an emulsion is used as the paint binder. These dispersions are prepared through emulsion polymerisation, a type of radical polymerisation. Styrene (sty), methyl methacrylate (MMA) and 2-ethylhexyl acrylate (2-EHA), are some of the monomers commonly used to form latexes (Negim, E. S. et al., 2016). A typical emulsion polymerisation formulation comprises mainly the monomers, water, surfactants and a water-soluble initiator. Most of the relatively hydrophobic monomers that are added dwell in reservoirs, as monomer droplets. Only some of such monomers are present in the micelles. Once an initiator is added to begin polymerisation, latex particles are generated via the capture of free radicals by monomer-swollen micelles, which propagate by reacting with the monomers (Chern, C. S., 2006). The final product is a dispersion of solid latex particles in water; in the form of a colloidal dispersion.

Fillers: These are granular solids that are added to paint to thicken the films, and to also provide it with structure and volume. It mainly reduces the cost while also imparting texture and hardness (Gürses, A. et al., 2016). Some examples include clays, calcium carbonate ($CaCO_3$) and fumed silica (SiO_2).

Pigments: These are also granular solids that help to provide opacity and colour to the paint. White pigments are generally used as the base. Most paints today frequently use titanium dioxide and fumed silica in formulations (Ahmed, N. M. et al., 2012). TiO_2 is commonly used due to its high refractive index of 2.71, scattering all wavelengths of visible light, providing paint with good hiding power and vibrancy. It is however very expensive. Thus, companies tend to include other pigments such as fumed silica to reduce the cost, though at the expense of a lower refractive index of 1.45. The hiding power of a material is related to the refractive index according to Fresnel's equations (for normal incidence) (Born, M., & Wolf, E., 1959).

$$R = \left| \frac{n_1 - n_2}{n_1 + n_2} \right|^2$$

Where R is the reflectance of light, T is the transmittance, n_1 and n_2 the refractive indices of the 2 mediums.

Given that $R + T = 1$, for light passing through air with a refractive index of 1, $R = \left(\frac{n-1}{n+1}\right)^2$. The higher the refractive index of the material *n*, the lower will be the reflectance, indicating a higher hiding power of the paint.

Additives: Additives are added in small amounts to help improve the paint's functionality. One such additive, dispersing agents, are added to paint to ensure stability of the pigments and fillers by adsorbing onto them when it is mixed with the latex. They deflocculate the solid particles, reducing the viscosity of the paint, which also

allows for more fillers to be added. Wetting agents are also added to help initiate the dispersing process by lowering the surface tension of water in the paint, to allow for wetting, where air surrounding the inorganic particles is now substituted by water. Rheology modifiers also help to improve the viscosity of paint for application, thickening it, while also improving their storage capacity, by preventing sedimentation of the pigments within the formulation (BASF, 2016). Defoamers are necessary in paints, in preventing bubble formation to provide an even surfaced paint. Anti-freeze additives are also added to prevent freezing of the paint in colder conditions. Even biocides must be added to prevent microbial deterioration, increasing paint shelf-life.

Coalescing agents: These agents are important in aiding latexes of high glass transition temperatures (T_g) with film formation, ensuring a smooth finish to the film. The stages of film formation can be broken into 3 main stages: evaporation & particle concentration, particle deformation, and lastly polymer chain interdiffusion. Upon application of the dispersion paint, the evaporation of water will lead to a reduction in volume; this is known as the concentration phase of the film formation process. This forces the latex particles to move together till repulsive forces – as a result of adsorbed surfactants, are overcome. This is the longest stage of the three, and ends once the polymer has reached 60-70% of volume fraction (full contact is achieved at 74%) (Steward, P.A, 2000). Next, once contact between the particles is made, deformation begins to via Van der Waals and capillary forces, filling in all voids left by the removal of water. Though close to achieving a homogenous film, with about 80% solid content, particles are still separated by their hydrophilic layers, and are hence still distinguishable (Chevalier, Y, 1992). The end of the deformation stage corresponds closely to the minimum film-formation temperature (MFFT) (Taylor, J. W, 2002), where the MFFT of a paint or coating is the lowest temperature at which it will uniformly coalesce when laid on a substrate as a thin film. As more water is removed from the system, by diffusing through surface polymeric sheets formed at this stage as suggested by Sheetz in a study on film drying (1965), the hydrophilic layers then break up to allow direct contact between the cores of neighboring particles. This then starts the last stage of film formation known as interdiffusion, where the core polymers are released from their initial confinement and allowed to diffuse throughout the film, entangling with one another till a continuous polymer matrix is formed; it is during this stage that the film gains its mechanical properties (Steward, P.A, 2000). Coalescing agents help in this stage by functioning as temporary plasticizers, dissolving polymers to lower their T_g below room temperature, such that polymer hardness which resists interdiffusion (associated with the T_g) can be decreased.

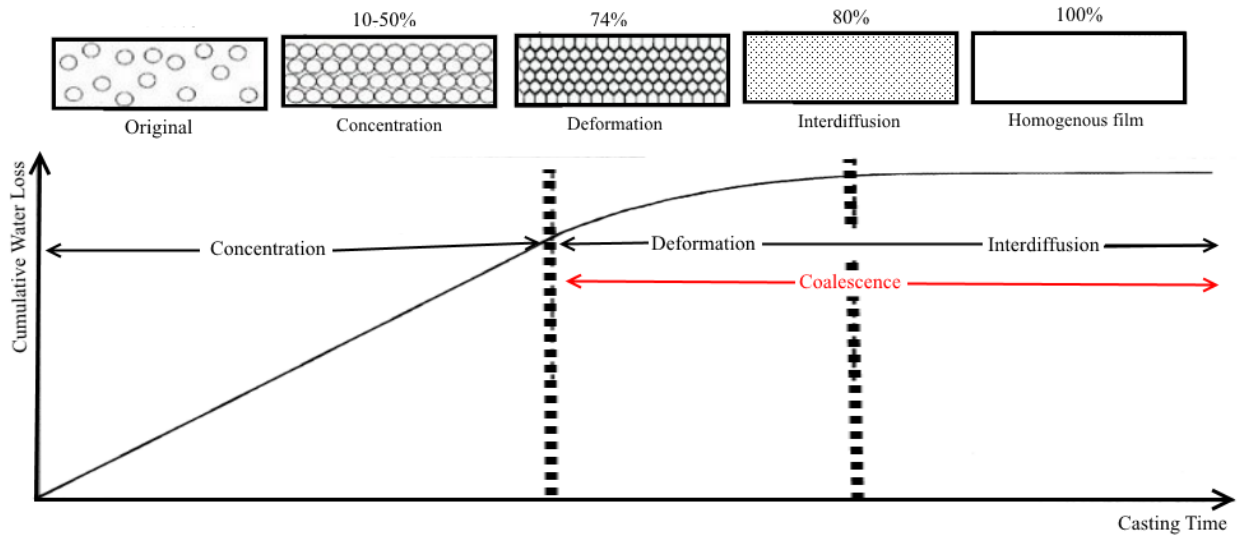

Figure 1. Structural transformations of a latex film while drying (Taylor, J. W, 2002) and a schematic plot of water loss against casting time (Steward, P.A, 2000)

However, since they have to evaporate off after coalescence, functioning as temporary plasticizers, VOCs are commonly chosen to be used as coalescing agents. This helps to reharden the film, by increasing the T_g. Even in labeled "VOC-free paints", Texanol ($C_{12}H_{24}O_3$) for example, which is the most commonly used coalescing agent, only has a boiling point of 254 °C - passing the VOC classification limit by a bare 4 °C (Eastman, 2004).

This project thus aims to provide an environmentally friendly alternative to VOCs, in order to develop a fully VOC free emulsion-based exterior coating. It is hypothesised that interactions between inorganic nanoparticles and the latex is possible, to create a jump in the glass transition temperature (T_g) of the nanocomposite, from a lower starting T_g; thus achieving a similar effect in drying during film formation. With a jump in T_g of the polymer, above room temperature, the polymers are able to transition from a rubbery or viscous state for

application to that of a hard glassy state for drying, as polymer chain mobility is restricted. Recent studies have shown that incorporation of SiO_2 show promise in increasing mechanical strength of composites. For example, PVA/SiO_2 composites improved the elastic modulus of composites at temperatures above 200 °C, in the rubbery state (Dodda, J. M, 2015), while others incorporated SiO_2 of 10nm in diameter in epoxy coatings, which were able to create an increase in T_g upon increasing loading from 1 wt% to 5wt% (Allahverdi, A, 2012). On the other hand, other studies on PEEK nanocomposites showed instead to have no effect, to even a slight decrease in T_g upon the incorporation of SiO_2 into the polymer systems. However, it is to be noted that these films contained high loadings of SiO_2, from 2.5 wt% to 10 wt% (Lai, Y. H.,, 2007).

Since SiO_2 is commonly used as a cheap option to pigments and fillers (inorganic components) in paints, for this investigation, fumed SiO_2 nanocomposites using a copolymer latex were synthesized. These nanocomposites were created using a casting approach. The storage modulus (E') which measures the stored energy and the loss modulus (E") which measures the dissipated energy, representing the elastic response and viscous portion respectively; were measured for the nanocomposites. Their ratios were then calculated as a loss tangent, tan δ. This will show the damping behavior of the nanocomposite materials and allow for the T_g to be analysed. The effect of loading and surface area of fumed SiO_2 on T_g of the nanocomposites was then investigated.

Storage Modulus: $E' = \frac{\sigma_0}{\varepsilon_0}\cos\delta$ Loss Modulus: $E'' = \frac{\sigma_0}{\varepsilon_0}\sin\delta$ Loss tangent: $\tan\delta = \frac{E''}{E'}$

Where ε is the the oscillatory force (stress) and σ is the resulting displacement (strain).

The thermal properties of the membranes were characterized using dynamic mechanical analysis (DMA) and a minimum film formation temperature bar. Paints were then formulated based on the results, tested on a substrate and underwent a water stain test.

2. Materials and Methods

2.1 Materials

Fumed SiO_2 of 10 nm and 200 nm in diameter were purchased from Sigma-Aldrich (USA). The copolymer latex that was synthesised by emulsion polymerisation consisted of the following monomers: Styrene (sty), Methyl Methacrylate (MMA), 2-Hydroxyethyl Acrylate (HEA) and Methacrylic acid (MAA) which were also purchased from Sigma-Aldrich (USA). For the paint formulation, wetting agents (Ecosurf BO-405), defoamer (Rhodoline DF6002), dispersants (Rhodoline 111) and thickener (Hydroxyethyl cellulose, HEC QP30000H) were all purchased from DOW (USA). The 30% ammonia solution, fillers (BYK Cloisite Na^+), pigments (TiO_2) and anti-freezing agent (propylene glycol, $C_3H_8O_2$) also used in paint formulation was purchased from Sigma-Aldrich (USA). All the chemicals were of analytical grade and used as received. Deionized (DI) water was utilized for all the membrane preparation experiments. All beakers and petri dishes (7.2 cm) used were cleaned with DI water and acetone, and dried in an oven overnight.

2.2 Preparation of copolymer latex

A total 200ml emulsion was prepared at 30% solid content, consisting of 60ml of monomers: Sty, HEA, MMA and MAA that were mixed according to a trade secret recipe. Sodium dodecyl sulfate (SDS) was used as a surfactant in this reaction. 4 wt% of surfactant and 2 wt% of sodium bicarbonate, which was used as a buffer for basic conditions, is first added to argon-bubbled water using a schlenk line. The mixture is then stirred within the double jacketed glass reactor and heated to 70 °C with a water circulator. Next, pre-dissolved ammonium persulfate (APS) initiator of 1 wt% is added to the mixture, followed by feeding of monomer mixtures into the solution at 0.2mL/min via a syringe pump. The reaction was allowed to stir for 24 hours to consume all the monomers. After the reaction was completed, the mixture is then filtered.

2.3 Preparation of films

The loading of fumed SiO_2 for sizes 200 nm and 10 nm were varied for a definite set of values, for a fixed amount of latex. A wide range of values from 0 wt% to 90 wt% was selected for calibration and it was found that for nanocomposites above 10 wt%, fracturing would occur, preventing the formation of smooth films for investigation. The nanocomposite membranes were prepared by the solution casting method, and the steps are as follows: The wt% of the 10nm fumed silica and the latex was varied for the various loadings. Dispersion was then carried out by placing the samples in an ultrasonic bath (Kodo, Korea) for 20 mins at room temperature. To

disperse the mixture further, using an Ultra-Turrax T-25 Digital Homogenizer by IKA, the composite was stirred at 6500 rpm for 3 mins. DI water was added in small amounts if the mixture was too viscous. The samples were then poured into petri dishes (7.2 cm) and placed in a vacuum oven at 65°C overnight till a solid composite film was cast. The same was replicated for 200 nm fumed silica.

Table 1. Nomenclature of materials

Sl No	Amount of SiO_2 (ø=10 nm) (g)	Amount of latex (g)	Sample name		Amount of SiO_2 (ø=200 nm) (g)	Amount of latex (g)	Sample name
1	0.00000	6	L/S 10 0 wt%		0	6	L/S 200 0 wt%
2	0.00361	6	L/S 10 0.2 wt%		0.00361	6	L/S 200 0.2 wt%
3	0.00723	6	L/S 10 0.4 wt%		0.00723	6	L/S 200 0.4 wt%
4	0.01087	6	L/S 10 0.6 wt%		0.01087	6	L/S 200 0.6 wt%
5	0.01452	6	L/S 10 0.8 wt%		0.01452	6	L/S 200 0.8 wt%
6	0.01818	6	L/S 10 1.0 wt%		0.01818	6	L/S 200 1.0 wt%
7	0.02186	6	L/S 10 1.2 wt%		0.02186	6	L/S 200 1.2 wt%
8	0.02556	6	L/S 10 1.4 wt%		0.02556	6	L/S 200 1.4 wt%
9	0.02927	6	L/S 10 1.6 wt%		0.02927	6	L/S 200 1.6 wt%
10	0.03299	6	L/S 10 1.8 wt%		0.03299	6	L/S 200 1.8 wt%
11	0.03673	6	L/S 10 2.0 wt%		0.03673	6	L/S 200 2.0 wt%
12	0.09474	6	L/S 10 5.0 wt%		0.09474	6	L/S 200 5.0 wt%
13	0.20000	6	L/S 10 10.0 wt%		0.20000	6	L/S 200 10.0 wt%
14	0.45000	6	L/S 10 20.0 wt%		0.45000	6	L/S 200 20.0 wt%
15	0.77143	6	L/S 10 30.0 wt%		0.77143	6	L/S 200 30.0 wt%
16	1.20000	6	L/S 10 40.0 wt%		1.20000	6	L/S 200 40.0 wt%
17	1.80000	6	L/S 10 50.0 wt%		1.80000	6	L/S 200 50.0 wt%
18	2.70000	6	L/S 10 60.0 wt%		2.70000	6	L/S 200 60.0 wt%
19	4.20000	6	L/S 10 70.0 wt%		4.20000	6	L/S 200 70.0 wt%
20	7.20000	6	L/S 10 80.0 wt%		7.20000	6	L/S 200 80.0 wt%
21	16.20000	6	L/S 10 90.0 wt%		16.20000	6	L/S 200 90.0 wt%

2.5 Characterisation

Dynamic Light Scattering (DLS): The dispersion of the latex was characterised by dynamic light scattering, and was measured for the latex particle size and zeta potential. This would help to indicate the latex particle size distribution of the system and ensure that a stable dispersion was formed. A zetasizer nano ZS (Malvern, UK) DLS machine was used.

Dynamic Mechanical Analysis (DMA): Viscoelastic behaviour of the latex/SiO_2 composite films were studied through DMA analysis. The complex modulus ($\varepsilon^*=\varepsilon'+ i\varepsilon''$) was measured by the resultant strain of applied certain sinusoidal force to the materials. The loss tangent ($\tan\delta$) was then calculated to correlate storage and loss modulus data which will show the damping (energy dissipation) behavior of the nanocomposite materials. The temperature dependence of the storage modulus was determined using a DMA 242 D/1/G (NETZSCH, USA). The width and thickness of the membrane samples were measured using Vernier calipers and a micrometer screw gauge respectively, before keying the values into the provided software by NETZSCH. All experiments of the nanocomposites were conducted in N_2 atmosphere with a flow rate of at 100cc/min and pressure of 0.5 bar. The frequency used was 1 Hz starting from -25 °C up to 70 °C with a heating rate of 10 °C/min.

Minimum Film Formation Temperature Bar (MFFT): The MFFT of the nanocomposites were characterised using a MFFT-90 bar (Rhopoint, UK). A nickel plated copper platen was cooled at one end and heated on the other. A temperature cursor was then used in conjunction with temperature sensors to indicate the MFFT of the sample tested, at the region where the film turned from cloudy to a clear continuous film. The flow rate of water for cooling was set to 4L/min and all films were checked for the MFFT after an hour to ensure thorough film formation. The temperature range was varied from -5°C to 50 °C for all composite samples.

3. Results and discussion

3.1 Dynamic Light Scattering

Before the nanocomposites were synthesised, it was important to ensure the stability of the dispersion of the latex. This was done through DLS runs on the copolymer latex which showed a mean zeta potential value of -30mV; no phase separation was also observed, indicating that the dispersion was highly stable (Figure 2). Size distribution of the latex particles was also narrow, when intensity was plotted against size, obtaining a Z-average of 42.47 nm in diameter, which indicated no signs of agglomeration (Figure 3).

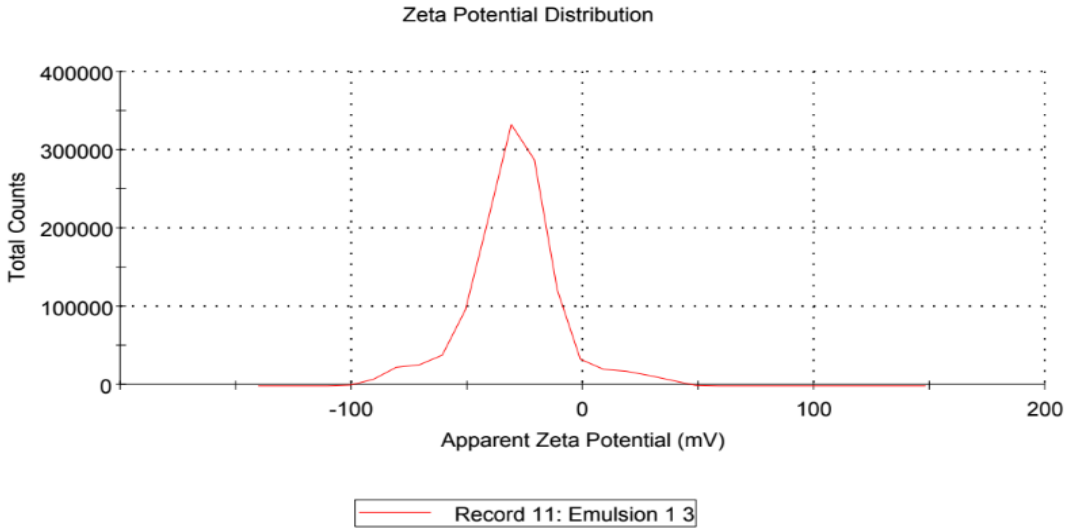

Figure 2. DLS Zeta potential report

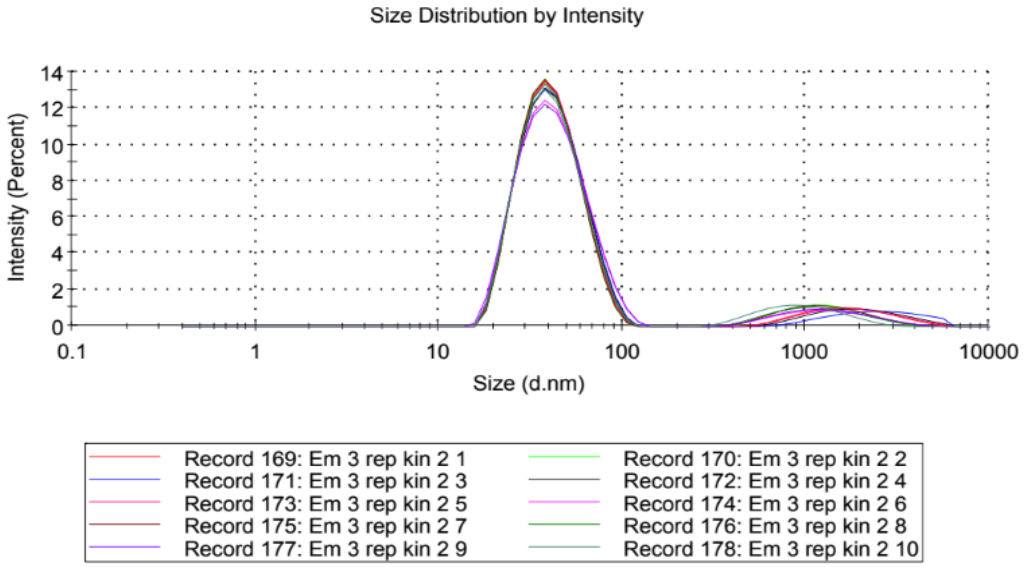

Figure 3. DLS Size Distribution Report by Intensity (Lines represent the replicated readings that were taken)

3.2 Dynamic Mechanical Analysis

DMA analysis was then performed to investigate the thermo-mechanical properties of the nanocomposite membranes, generally recognized to be sensitive to molecular motions and useful for evaluating subtle transitions occurred in a polymeric system (Chen, K., 2014). By calculating the ratio between the loss and storage modulus tan δ and plotting that as a function of temperature (Figures 4 & 5), the T_g, coresponding as a peak in the plots of the Latex/SiO_2 was calculated. It was observed that the latex/SiO_2 (ø=10 nm) composites showed T_g values of 37.7, 42.0, 48.8, 40.8, 43.4, 43.2, 41.2, 40.3, 39.9, 40.4, 39.9, 38.6, 37.7 °C for the latex and 0.2, 0.4, 0.6, 0.8, 1, 1.2, 1.4, 1.6, 1.8, 2, 5, 10 wt% SiO_2 (ø=10 nm) loaded latexes respectively (Figure 6).

The T_g increased with increasing loading of SiO_2 in all of the composites and becomes maximum at 0.4 wt % SiO_2 loading which resulted in the highest T_g (48.8 °C). Higher loading of SiO_2 caused a gradual decrease in T_g of the composite. A similar trend is observed for 200 nm sized SiO_2 particles where the T_g calculated from tan δ was observed to be 37.7, 37.6, 40.1, 40.8, 41.0, 45.8, 46.2, 44.6, 40.4, 40.2, 39.1, 37.7, 39.4 °C for 0.2, 0.4, 0.6, 0.8, 1, 1.2, 1.4, 1.6, 1.8, 2, 5, 10 wt% SiO2 (ø=200 nm) loaded latexes respectively (Figure 7). The T_g also increased initially, reaching a maximum at 1.2 wt% (46.2 °C), before gradually decreasing.

Hence it is clear that immobilization of the copolymer chains had occurred at lower loadings of the SiO_2 nanoparticles. This increase in T_g values to a maximum can be attributed to the physical interaction of copolymer chains and the surface functionality of the SiO_2 nanoparticles due to hydroxyl groups, which immobilised the free movement of the copolymer chains. Yet, it is also important to note that by incorporating SiO_2 nanoparticles into the latex, the free volume of the copolymer chains will be increased, imparting a negative effect on the T_g improvement of the composite materials. This is according to the Flory-Fox equation where an increase in free volume, represented by the empirical parameter *K*, for a constant molecular weight, will decrease the glass transition temperature of the composite. For higher loadings, nanoparticles have a much higher tendency to create agglomerates. At lower wt% loadings however, this effect was not as potent due to the fact that the SiO_2 nanoparticles were able to better accommodate themselves within the matrix. This ensured the maximum probability for physical interaction with the copolymer chains, which played a vital role in T_g increment of the nanocomposites. At further higher wt% loading of SiO_2 nanoparticles, the increase in free volume of the polymer chains outweighed the physical interactions between the latex and SiO_2 nanoparticles, which led to the decreasing trend in T_g. As such, it can be concluded that SiO_2 is able to enhance the T_g of the composite through interfacial physical interaction, allowing it to reach a maximum up to a certain extent, varying based on the loading of nanoparticles incorporated.

By comparing the two composites of different silica loadings, the effect of surface area on T_g can also be investigated. For the same latex, composite L/S 200 1.2 wt% required higher loadings of SiO_2 than L/S 10 0.4 wt% before the maximum T_g was attained (Figures 4 & 5). It can also be observed that the T_g values obtained for 10nm composites were generally higher than that of the 200nm composites. This might seem unexpected since 200nm nanoparticles being larger in size, with a significantly larger surface functionality are expected to have greater interaction than that of the 10nm nanoparticles. However, it is important to note that the nanoparticles are actually interacting with latex particles with an average diameter of 42.47 nm as shown previously in DLS scans (Figure 3). Therefore, 200nm SiO_2 nanoparticles being comparatively larger in size than the 10nm SiO_2 nanoparticles were less able to rearrange itself within the polymer matrix, having a low surface to volume ratio, and could not fully maximize interfacial interactions with the latex particles, and thus required higher loadings before interfacial interactions could be maximised. The 200nm nanoparticles even at higher loadings still obtained generally lower T_g values due to their sheer size in comparison to the latex, which left many functional groups unutilised and thereby had less extensive bonding. This implies that 10nm nanoparticles are better suited at enhancing the T_g.

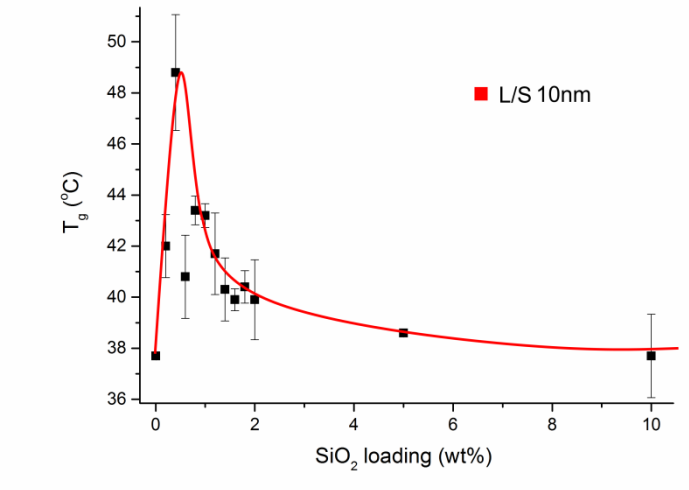

Figure 4. Plot of T_g against SiO_2 loading for Latex/SiO_2 (ø=10 nm) composite materials

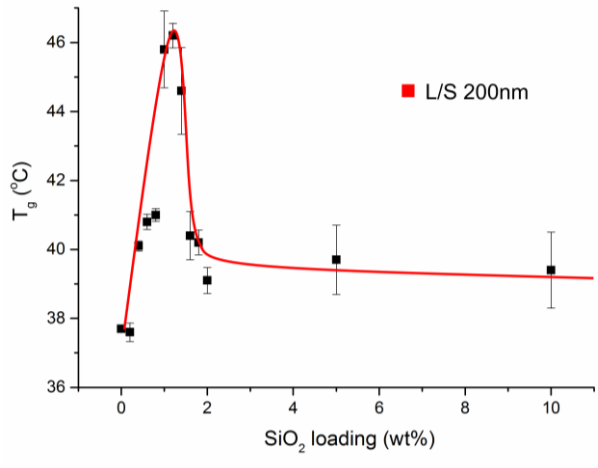

Figure 5. Plot of T_g against SiO_2 loading for Latex/SiO_2 (ø=200 nm) composite materials

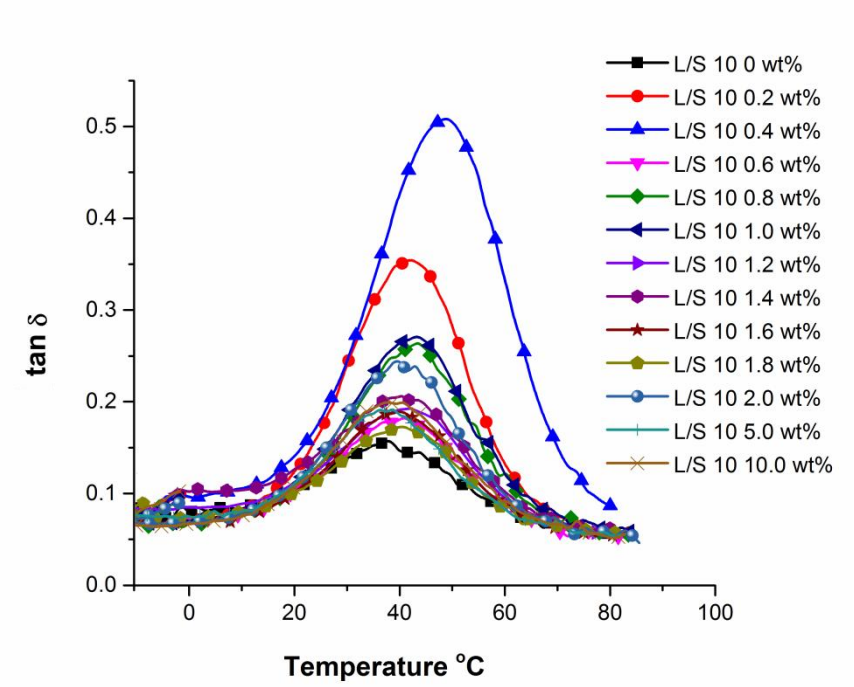

Figure 6. The plot of tanδ against temperature for the latex and the corresponding Latex/SiO_2 (ø=10 nm) composite materials, peaks are indicative of the T_g

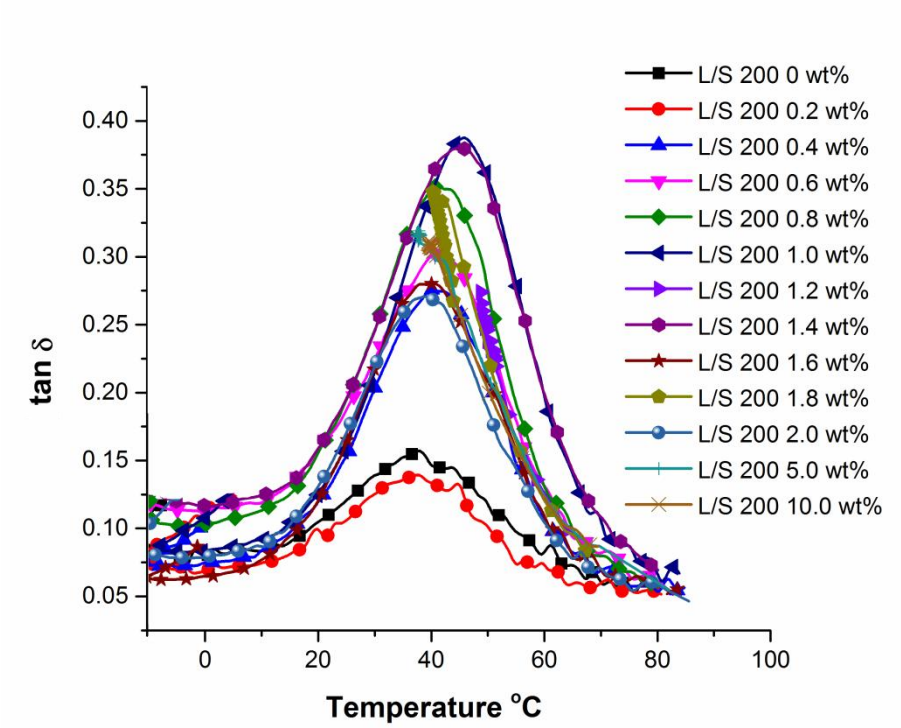

Figure 7. The plot of tanδ against temperature for the latex and the corresponding Latex/SiO_2 (ø=200 nm) composite materials, peaks are indicative of the T_g

3.3 Minimum Film Formation Temperature

The MFFT of the nanocomposites were also analysed, comparing between the latex and samples L/S 10 0.4 wt% and L/S 200 1.2 wt% which showed the maximum T_g values for their respective sizes. The MFFT values obtained were 9.9 °C, 14.7 °C and 17.9 °C and respectively. The MMFT was obtained by placing the

temperature cursor directly onto the region (Figure 8) which bounded the cloudy, cracked film (Figure 9) from the clear and continuous film. Although the addition of SiO_2 into the latex did raise the MFFT, the nanocomposites still maintained a MFFT below room temperature; ensuring that upon drying, a smooth film will be formed. This was achieved despite the increased segmental mobility of the silica polymer interphase, indicating that water could have helped in plasticization of the polymers, allowing for better interdiffusion during coalescence before it evaporated off. Since L/S 10 0.4 wt% had a lower MFFT than L/S 200 1.2 wt%, all while providing a better increase in the T_g at a lower loading, it was more desirable to be chosen for the paint formulation, due to its cost-effective benefits.

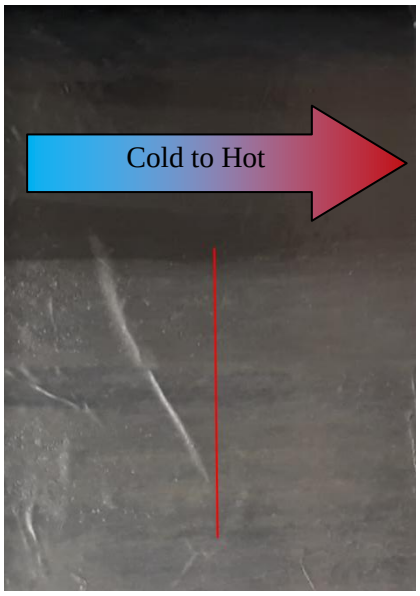

Figure 8. MFFT determining boundary, between cracked (left) film and smooth film (right) of latex

Figure 9. Cracked and cloudy film of latex without the addition of SiO_2

3.4 Paint formulation

Paint components were mixed in 2 stages, namely the mill base stage and the let down stage. During the grind mill base stage, inorganic components were first mixed using a basket mill (DISPERMAT, Germany). As ingredients were added into the basket mill, stirring was maintained at 400 rpm. Once all ingredients were added into the mill, the speed was increased to 2000 rpm to ensure a thorough mix. After each hour, 1 ml of the mix was taken out to be checked on a grind gauge to determine if the mill base stage was completed. The paint was placed onto a fineness grind gauge 0-199UM GROOVES (Elcometer, UK) at one end, and spread across the gauge toward the other end. The section where the paint begins to fade off was then observed, where if the rough section (indicative of coarse particles) was below the 30 µm mark (Figure 10), that meant that the pigment mix was grounded finely enough to be mixed with the latex component. During the let down stage, the latex was then added into the mixture and stirred at 800 rpm for 3hrs. Two recipes were made, one being a blank without the addition of SiO_2 (Table 2) and one with the added SiO_2 (ø=10 nm) (Table 3).

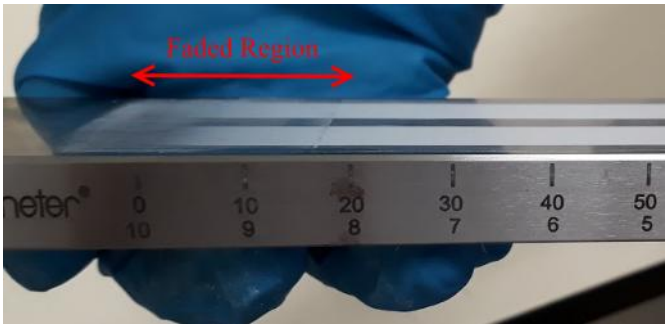

Figure 10. Mill base tested on a grind gauge, agglomerated particles were grounded finely below the 30 µm mark

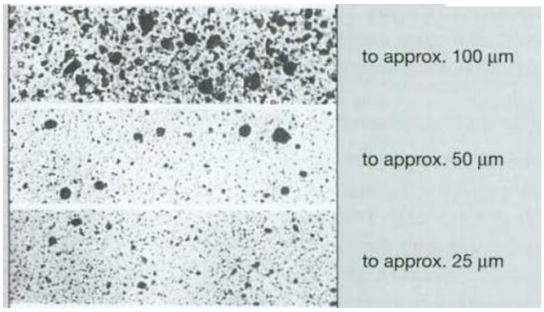

Figure 11. Scale for visual assessment of the fineness of grind (Oyarzún, J. M., 2000)

Table 2. Recipe 1(Blank)

Mill Base			
Sl No	Component	Mass (g)	Function
1	Water	216	Solvent
2	HEC QP30000H	0.75	Thickener
3	TiO_2	70	Pigment
4	BYK Cloisite Na^+	115	Filler
5	SiO_2 (ø=10 nm)	0	Mechanical strength and T_g improvement
Let Down			
6	Latex	142	Binder
7	Ammonia (30%)	10	Balance the pH of MAA, also helps as a biocide
8	Rhodoline 111	2	Dispersant
9	Ecosurf BO-405	1	Wetting Agent
10	Propylene Glycol	5	Anti-freezing agent
11	Rhodoline DF6002	0.5	Defoamer

Table 3. Recipe 2 (SiO_2 loaded)

Mill Base			
Sl No	Component	Mass (g)	Function
1	Water	216	Solvent
2	HEC QP30000H	0.75	Thickener
3	TiO_2	70	Pigment
4	BYK Cloisite Na^+	115	Filler
5	SiO_2 (ø=10 nm)	60	Mechanical strength and T_g improvement
Let Down			
6	Latex	142	Binder
7	Ammonia (30%)	10	Balance the pH of MAA, also helps as a biocide
8	Rhodoline 111	2	Dispersant
9	Ecosurf BO-405	1	Wetting Agent
10	Propylene Glycol	5	Anti-freezing agent
11	Rhodoline DF6002	0.5	Defoamer

3.5 Paint on substrate

Both paints were tested on an aluminum substrate, applied using a paint applicator. The paints upon application dried within an hour at room temperature, and after drying had a smooth texture when touched, with no visible bumps seen. The smooth formation of the film can be attributed to the low MFFT values when measured, which allowed for coalescence to occur without issue. However, although the film was smooth, the blank film still showed cracking while the loaded film did not. (Figure 12) This reinforces the point that the SiO_2 nanoparticles were indeed able to enhance the T_g, leading to optimum mechanical properties in terms of the tensile strength of the material, due to the interfacial hydrogen bonding interactions between the surface hydroxyl groups of SiO2 and the hydrophilic latex components. Due to the TiO_2 added, the paints also appeared vibrant, synonymous to white paint regularly seen on walls.

Figure 12. Comparison of paint films after drying, blank film (left) showed cracking while loaded film (right) did not

3.6 Water Stain Mark Test

As we are focusing on exterior coatings, it was also highly important to ensure that the paints formulated would not leave any stains upon contact with water. 1ml of water was placed onto both samples which were wiped off after 15 mins. Now water marks were observed in component. As such, it could be concluded that the water soluble monomers MAA, containing carboxyl groups (COOH), were incorporated into the latex did not wash away nor had any wetting effect with water. This also helps to show that the physical interactions between the hydrophilic regions of the latex and the hydroxyl functionality of the inorganic particles were fully maximized as a result.

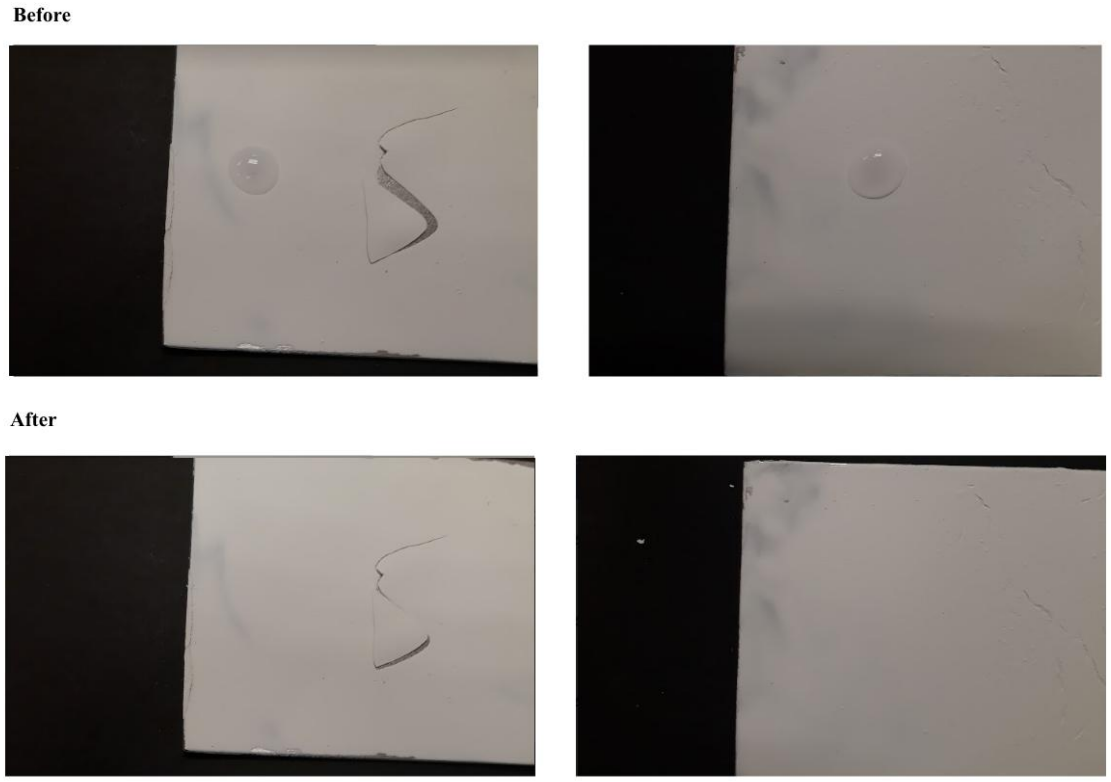

Figure 13. Comparison of paint films after water was added onto both the blank film (left) and loaded film (right), no stains observed

4. Conclusion

From DMA analysis, it can be concluded that inclusion of SiO_2 nanoparticles are able to increase the T_g to a maximum at low loadings, peaking before gradually decreasing at higher loadings. The smaller nanoparticles (ø=10 nm) were also observed to have a better enhancement in T_g as opposed to the larger nanoparticles (ø=200 nm), requiring lesser loadings of fumed silica (difference of 0.8 wt% loading) for the maximum to be achieved, in addition to having a range of higher T_g values. Furthermore, smaller nanoparticles were also observed to have lower MFFT values for films formed, below room temperature, which makes it both highly reliable and cost beneficial to be incorporated in paint formulation. Extensive bonding between the latex and inorganic particles were maximized evident from the testing through water mark stain tests, in which both paints were unaffected by water even though water soluble monomers were used. With regard to the final dried films, SiO_2 loaded paint showed no cracks at all, proving better mechanical strength due to the addition of SiO_2 particles, which interacted with polymer chains, precipitously decreasing the cooperative motion of the matrix polymer. From this investigation, we have observed that even though the T_g of the nanocomposites were increased, a smooth film was still able to be formed. This implies that SiO_2 could be involved in a new mechanism, by playing a huge factor in aiding the coalescing process during interdiffusion, through interfacial interactions with polymers. Water could have also possibly provided a hydroplasticizing effect (Sperry, P. R, 1994), aiding in coalescence before being evaporated off, which explains the low MFFT values obtained. From this investigation, it can be concluded that a smooth exterior coating can in fact be formed through a jump in T_g, achieved through the addition of SiO_2 particles, with high mechanical strength, while still obtaining an MFFT below room temperature. This paves the way for further study on silica nanocomposites used in paint formulation, to provide an alternative mechanism to develop environmentally friendly, VOC-free exterior paint coatings.

For future work, further tests on paint formulations can be conducted, in testing weatherability, durability, hiding properties and tensile strength in different environments. Fourier-transform infrared spectroscopy (FTIR) can also be conducted to better understand the physical interactions between polymer and inorganic particles. The type of silica can also be varied, testing porous silica for example which has a high surface area to volume ratio could allow for increased interfacial interaction and mechanical properties in paint.

5. References

[1] Directive, E. U. (2004). Directive 2004/42/CE of the European Parliament and of the Council of 21 April 2004 on the limitation of emissions of volatile organic compounds due to the use of organic solvents in certain paints and varnishes and vehicle refinishing products amending Directive 1999/13/EC. *Official Journal of the European Union L*, *143*.

[2] Volatile Organic Compound Control Regulations | Ground-level Ozone | New England | US EPA. (2017, April 10). Retrieved August 20, 2017, from https://www3.epa.gov/region1/airquality/voc.html

[3] Buday, M., Cater, F., Foulkes, S., Prakash, N. S. O., & Wilson, D. (2010). Sherwin Williams: Splashing into the low VOC paint market. Published by GlobaLens, a division of the William Davidson Institute at the University of Michigan. Case 1-428-993. 1 – 16.

[4] de Hek, H., Zabel, K. H., & Geurink, P. J. A. (1998). Accepting the VOC-challenge: Recent developments in architectural coatings. Surface Coatings Australia, 35, 14 – 22

[5] Volatile Organic Compounds' Impact on Indoor Air Quality. (2017, April 19). Retrieved July 13, 2017, from https://www.epa.gov/indoor-air-quality-iaq/volatile-organic-compounds-impact-indoor-air-quality#Health_Effects

[6] PCI (n.d.). What is Powder Coating? Retrieved December 13, 2017, from http://www.powdercoating.org/page/WhatIsPC

[7] *Ian J. Rogan*, I. J. (n.d.). (2002) Acrylic paint. Retrieved December 12, 2017, from http://www.cool.conservation-us.org/byform/mailing-lists/cdl/2002/1361.html

[8] Zhu, A., Cai, A., Yu, Z., & Zhou, W. (2008). Film characterization of poly(styrene-butylacrylate-acrylic acid)–silica nanocomposite. Journal of Colloid and Interface Science,322(1), 51-58. doi:10.1016/j.jcis.2008.02.014

[9] Water based vs Solvent based. (n.d.). Retrieved December 12, 2017, from http://www.paintquality.com/en/understanding-paint/water-based-vs-solvent-based

[10] Shawn Cole (n.d.). (2011) Retrieved December 12, 2017, from http://colerepair.com/Latex%20paint%20vs%20oil%20based%20paint

[11] lrich Poth, "Drying Oils and Related Products" in Ullmann's Encyclopedia of Industrial Chemistry Wiley-VCH, Weinheim, 2002. doi:10.1002/14356007.a09_055

[12] Negim, E. S., Aisha, N., Mun, G. A., Iskakov, R., Irmukhametova, G. S., & Sakhy, M. (2016). Preparation and Characterization of Acrylic Primer for Concrete Substrate Application. *International Journal of Polymer Science, 2016*.

[13] Chern, C. S. (2006). Emulsion polymerization mechanisms and kinetics. *Progress in polymer science*, *31*(5), 443-486.

[14] Gürses, A., Açikyildiz, M., Güneş, K., & Gürses, M. S. (2016). *Dyes and pigments*. New York, NY: Springer.

[15] Ahmed, N. M., & Abdel-Fatah, H. T. M. (2012). The role of silica fume pigments in corrosion protection of steel surfaces. In *Recent Researches in Corrosion Evaluation and Protection*. InTech.

[16] Born, M., & Wolf, E. (1959). *Principles of optics: Electromagnetic theory of propagation interference and diffraction of light*. London: Pergamon Press.

[17] SE, B. (2016). *Practical Guide to Rheology Modifiers*.

[18] Steward, P. A., Hearn, J., & Wilkinson, M. C. (2000). An overview of polymer latex film formation and properties. *Advances in colloid and interface science*, *86*(3), 195-267.

[19] Chevalier, Y., Pichot, C., Graillat, C., Joanicot, M., Wong, K., Maquet, J., ... & Cabane, B. (1992). Film formation with latex particles. *Colloid & Polymer Science*, *270*(8), 806-821.

[20] Taylor, J. W., & Klots, T. D. (2002). Applied approach to film formation: The glass transition temperature evolution of plasticized latex films. *European coatings journal*, (6), 38-54.

[21] Sheetz, D. P. (1965). Formation of films by drying of latex. *Journal of Applied Polymer Science*, *9*(11), 3759-3773.

[22] Eastman says European Union action gives texanol coalescent non-VOC status. (2004). *Pigment & Resin Technology*, *33*(5). doi:10.1108/prt.2004.12933eab.011

[23] Dodda, J. M., Bělský, P., Chmelař, J., Remiš, T., Smolná, K., Tomáš, M., ... & Kadlec, J. (2015). Comparative study of PVA/SiO2 and PVA/SiO2/glutaraldehyde (GA) nanocomposite membranes prepared by single-step solution casting method. *Journal of materials science*, *50*(19), 6477-6490.

[24] Allahverdi, A., Ehsani, M., Janpour, H., & Ahmadi, S. (2012). The effect of nanosilica on mechanical, thermal and morphological properties of epoxy coating. *Progress in Organic Coatings*, *75*(4), 543-548.

[25] Lai, Y. H., Kuo, M. C., Huang, J. C., & Chen, M. (2007). On the PEEK composites reinforced by surface-modified nano-silica. *Materials Science and Engineering: A*, *458*(1), 158-169.

[26] Chen, K., Tian, C., Lu, A., Zhou, Q., Jia, X., & Wang, J. (2014). Effect of SiO2 on rheology, morphology, thermal, and mechanical properties of high thermal stable epoxy foam. *Journal of Applied Polymer Science*, *131*(7).

[27] Oyarzún, J. M. (2000). Pigment Processing. *Druckerei Hubert & Co., Gottingen. ISBN 3-87870-556*, *5*.

[28] Sperry, P. R., Snyder, B. S., O'Dowd, M., & Lesko, P. M. (1994). Role of water in particle deformation and compaction in latex film formation. *Langmuir*, *10*(8), 2619-2628.